



Article

Long-Term Deformations and Mechanical Properties of Fine Recycled Aggregate Earth Concrete

Hassan Fardoun , Jacqueline Saliba * , Jean-Luc Coureau, Alain Cointe and Nadia Saiyouri

Institut de Mécanique et d'Ingénierie (I2M), CNRS, Esplanade des Arts et Métiers, Université de Bordeaux, UMR 5295, 33405 Talence, France

* Correspondence: jacqueline.saliba@u-bordeaux.fr

Abstract: Earth-based materials are currently receiving high attention, as they are considered as sustainable. In addition, the reuse of waste materials and more particularly recycled aggregates can boost circular economy while reducing landfilling and mineral resource depletion. Incorporating recycled aggregates in earth concrete can be an innovative way to valorize them. However, investigations are required concerning their long-term behavior. Such an aspect is more important when fine recycled aggregates are considered. In this paper, the vulnerability to long term deformations of natural sand (NS) and recycled sand (RS) earth concrete mixtures is examined under real exposure conditions. Autogenous shrinkage, drying shrinkage, basic creep and drying creep of the different mixtures were monitored for a period of two months. Specimens were then subjected to compressive tests in order to evaluate their residual strength. Furthermore, the destructive tests were monitored in parallel with the acoustic emission (AE) technique. The results show an increase in the rate of drying creep and shrinkage for RS earth concrete mixtures. In addition, NS and RS earth concrete mixtures subjected to drying, with and without loading, reported a strength development in comparison to the reference mixtures. However, the Young's modulus reported its lowest value for drying shrinkage of both mixtures. Regarding the AE technique, the distribution of its activity reflected the higher rate of damage of dried specimens in the pre-peak region.

Keywords: earth concrete; autogenous shrinkage; drying shrinkage; basic creep; drying creep; recycled sand; acoustic emission



Citation: Fardoun, H.; Saliba, J.; Coureau, J.-L.; Cointe, A.; Saiyouri, N. Long-Term Deformations and Mechanical Properties of Fine Recycled Aggregate Earth Concrete. *Appl. Sci.* **2022**, *12*, 11489. <https://doi.org/10.3390/app122211489>

Academic Editor: Cesare Oliviero Rossi

Received: 22 October 2022

Accepted: 8 November 2022

Published: 12 November 2022

Publisher's Note: MDPI stays neutral with regard to jurisdictional claims in published maps and institutional affiliations.



Copyright: © 2022 by the authors. Licensee MDPI, Basel, Switzerland. This article is an open access article distributed under the terms and conditions of the Creative Commons Attribution (CC BY) license (<https://creativecommons.org/licenses/by/4.0/>).

1. Introduction

Carrying out construction with earth is an ancient building approach that dates back thousands of years, with different possible techniques, such as wattle and daub, cob, rammed earth and compressed earth block [1]. Earth construction materials are very interesting because of their low cost, recyclability and their limited energy consumption. In addition, they possess good thermal and insulation properties compared to normal concrete with sufficient mechanical strength [2]. A new earth construction material designed to be pourable, called earth concrete, has been recently considered [3–5].

On the other hand, the increasing construction works, continuous industrial development, infrastructure activities and residential market growth generate a huge amount of construction and demolition waste (CDW). CDW includes the waste generated from construction and demolition of buildings and infrastructure, in addition to road planning and maintenance. Over 10 billion tons of CDW are produced globally each year [6]. The European Union (EU) contributes to about 1 billion ton annually [7]. Kabirifar et al. [6] reported an overall 88–90% of recovery rate of CDW in EU in 2018. An improvement has been noticed compared to past years. Croatia, for instance, achieved a recovery rate of 2% in 2010, and has reported a value of 78% in 2018. The Netherlands continues to attain a 100% of recovery rate since 2010 due to its policy that considers such waste as a

base in road construction [8]. However, new markets need to be developed for an effective circular economy and a sustainable development of the construction industry while reducing the environmental impact of concrete [2]. Fine recycled aggregate or recycled sand (RS) accounts for about 50% of CDW [9,10]. The construction activities that involve concrete are numerous; however, RS is still applied only at a concrete laboratory scale. This is due to the fact that RS is generally porous and of high water absorption capacity, which negatively affects the mechanical and durability properties. In fact, the lack of standards can be behind the restriction of RS applications at construction sites [11]. Nevertheless, the consideration of RS as earth material component may still yield satisfactory results [2,11]; thus, this may permit to consider earth materials as alternative market for RS. Moreover, it would be interesting to assess the combination of RS as it is porous and clay constituted of fine particles which can have an important potential for energy conservation in buildings as it may reduce the thermal conductivity in addition to the reduction of CO₂ emissions and cost [2,12].

In this study, RS earth concrete mixture has been tested and compared to the behavior of NS earth concrete mixtures. More particularly the long-term deformations have been considered. In fact, few studies have been conducted in the literature on the effect of RS on mechanical properties and long-term deformations of earth concretes [12]. The structures are subjected to different mechanical loadings in addition to temperature and humidity variations during their lifetime [13–15]. Autogenous shrinkage and drying shrinkage are a result self-desiccation and drying, respectively [16,17]. The capillary pressure, disjoining pressure, surface tension and interlayer water theory may be behind such deformations. In normal concrete, a 66–83% decrease and 15–80% increase would be generally reported for the complete replacement of natural aggregate (NA) by recycled aggregate (RA) for autogenous and drying shrinkage, respectively [18,19]. In earth concrete, Kanema [20] reported swelling rather than shrinkage up to 200 $\mu\text{m}/\text{m}$ for autogenous assessment and a decrease of drying shrinkage from 2000 $\mu\text{m}/\text{m}$ to almost 1200 $\mu\text{m}/\text{m}$ when 31% of NA are replaced by RA.

In soils, the physical origin of creep is due to the primary consolidation process, which concerns the change in volume due to the dissipation of free water under applied stress and to the secondary compression process, which is the deformation under constant effective stress mainly due to the viscous behavior of the solid skeleton [21]. The occurrence of creep in soils can be due to the breakdown of interparticle bond, jumping of molecule bonds, sliding among particles, water flow in a double pore system, and structural viscosity [22]. Regarding the creep in concrete (as cement is an earth concrete component), the applied theories such as consolidation, seepage, bond breakage, and others are originally linked with soil and clay. Furthermore, they are all connected and involve water movement.

The sum of elastic strain, basic creep in addition to autogenous shrinkage and drying shrinkage, results generally in a total deformation less than that obtained, at simultaneous drying, from a loaded drying specimen. This difference or additional strain is known as drying creep or Picket's effect. The extended microprestress-solidification theory (XMPS) is allegedly to properly estimate the basic and drying creep in normal concrete. XMPS revealed that the viscosity of creep is significantly reduced by the existence of a water layer between the planer walls of C-S-H. Moreover, as the water layer moves, the effective viscosity of slip between the solid surfaces decreases [23,24]. In addition to such intrinsic effects, structural effects can contribute to the additional strain which is represented most importantly by the microcracking effect [25]. For complete replacement of NA by RA, normal concrete would generally report 25–100% creep increase [26]. To our knowledge, few papers were dedicated on the creep of earth construction materials or the effect of RS on creep of these materials [27].

Thus, studies investigating the long-term deformations at environments possessing variations in relative humidity are required for earth construction materials. In the following study, to the aim is to assess the complete replacement of NS by RS on the long-term deformations of earth concrete under real exposure curing conditions. Specimens were

then subjected to compressive tests in order to evaluate the residual mechanical properties, i.e., compressive strength and Young's modulus. Furthermore, the rupture tests were monitored in parallel with acoustic emission (AE) technique to better understand the fracture behavior [13–15,28].

2. Experimental Program

2.1. Materials

Artificial mixtures have been adopted in order to assess the effect of RS explicitly. In this case, 30% of kaolinite clay is mixed with 70% of NS in order to form NS earth concrete mixture from one side and with 70% of RS to form RS earth concrete mixture from other side. Kaolinite, a non-swelling clay, was used in order to reduce the volumetric change. Sieving was adopted for particles of diameter greater than 0.08 mm [29] while sedimentation was considered for the finer ones [30]. The tests displayed a 52.84% and 32.81% of liquid limit and plastic limit, respectively.

In this case, 9% of cement of the dry components mass (clay + aggregate) was added to all mixtures. Though it is not a low percentage, it is required to reach a certain compressive strength in earth concrete at early age in order to be able to remove the formwork board at early age and for durability purposes. The pure Portland cement CEM 1 (52.5 N PM-CP2) composed mainly of clinker was considered in order to prevent the effect of additional components [31]. The Tempo 10 superplasticizer was also added as a water reducing admixture. The dry components were first introduced into a blender and mixed for 5 min in order to obtain a homogeneous mixture. Next, water in addition to Tempo10 was progressively added in order to ensure similar workability values.

2.2. Mix Design

RS, which showed 14.6% water absorption capacity according to drying porous media [2], was 80% pre-saturated by putting the RS in containers and adding the amount of water 24 h prior to mixing. When dealing with RS, the term water is generally replaced by effective water (w_{eff}). In normal concrete, such a term is considered to be the total water minus the water required for the recycled aggregate. Herein, for earth concrete, w_{eff} could be considered as the total water (w_T) minus the water required for RS (w_{RS}) and that required for clay (w_{cl}). The equations of w_{RS} and w_{cl} are presented in Equations (1)–(3).

$$w_{eff} = w_T - (w_{RS} + w_{cl}) \quad (1)$$

$$w_{RS} = (w_{sat} * \frac{w_{ARS}}{100} * RS) - (\frac{w_{cRS}}{100} * RS) \quad (2)$$

$$w_{CL} = (\frac{W_{ll}}{100} * C) - (\frac{w_{cCL}}{100} * C) \quad (3)$$

where:

C is clay amount, RS is recycled sand content, w_{sat} is the saturation degree of RS, w_{ARS} and w_{ANS} are the water absorption of RS and NS, respectively, w_{cRS} is the water content of RS, w_{ll} is the liquid limit of clay, and w_{cCL} is the water content of clay.

The water required for RS pre-saturation occupies volume. Accordingly, a reduction in the number of other components of the RS earth concrete mixture is mandatory. Table 1 presents the parameters' values (where w_{cNS} is the water content of NS and Table 2 presents the mix designs). It can be noticed that a higher amount of effective water was required in the recycled sand mixture to reach similar workability compared to the natural sand one.

Table 1. The parameters' values.

w_{ll}	w_{cCL}	w_{ARS}	w_{cRS}	w_{ANS}	w_{cNS}
52.84%	0.5%	14.6%	2.58%	1.02%	0.05%

Table 2. Mix design.

Components (kg/m ³)	Clay (C)	Sand	Cement	w_{eff}	Superplasticizers
NS mixture	440	1026	132	140	1.32
RS mixture	366	855	110	177	1.32

2.3. Experimental Procedure

In this case, 12 cylinders of size $\text{Ø}11 \times 22 \text{ cm}^3$ were casted in order to measure in parallel the mass loss, the autogenous shrinkage, the drying shrinkage, the basic creep and the drying creep for each mixture. The specimens were conserved first in a climate-controlled chamber at a relative humidity (RH) of 50% ($\pm 5\%$) and at a temperature of 20 °C ($\pm 2 \text{ °C}$) with no exchange of water.

2.3.1. Shrinkage and Creep Measurements

The specimens were put outdoors starting from day 28. The temperature and RH were measured throughout the tests. The mass loss was also monitored in parallel for each mixture. Four specimens of each mixture were subjected to shrinkage and creep. For autogenous shrinkage and basic creep tests, the exchange of moisture was prevented by a double layer of self-adhesive aluminum paper. Basic and drying creep tests were conducted by using an electromechanical machine at a loading rate of 70% of the maximum stress of the reference mixtures. Note that the compressive tests carried out at the age of 28 days on the reference specimens yielded a peak stress of 2 MPa and 0.9 MPa for NS and RS specimens, respectively. Two rings were fixed on the specimens with three screws and three LVDT sensors, with an accuracy of $3 \text{ }\mu\text{m}$ placed at 120° for creep deformation measurement (Figure 1a). The relative displacement between the two sections was measured on a base of 80 mm at the central zone and the mean value was considered. A ball joint was designed to compensate any defects and avoid possible bending. The longitudinal deformation due to shrinkage was measured using one LVDT sensors (Figure 1b).

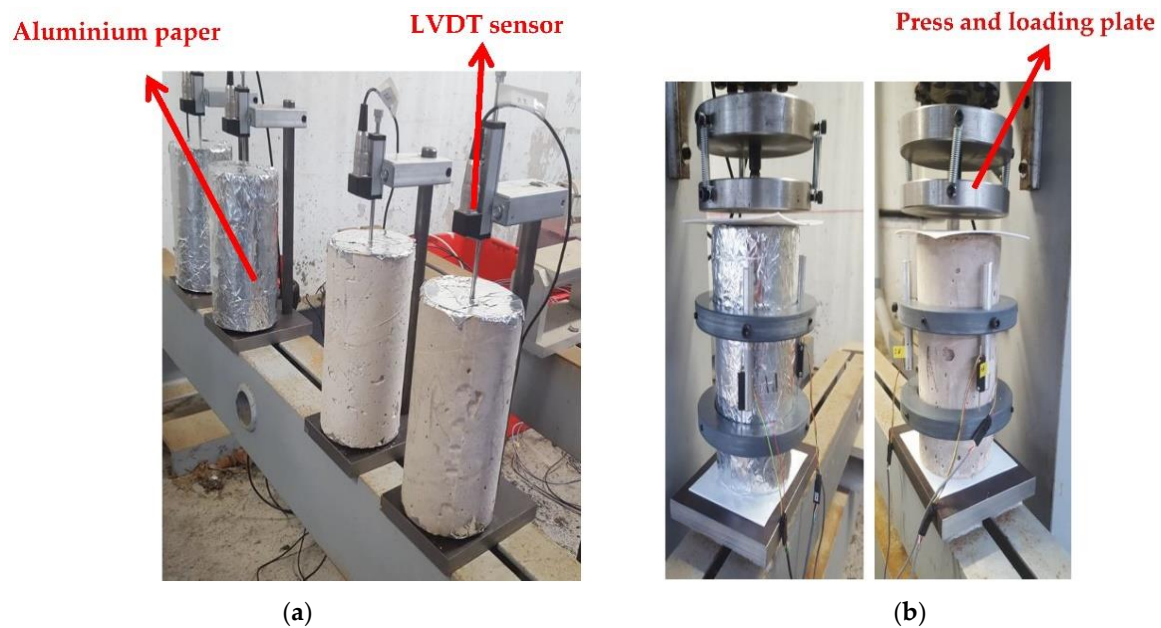


Figure 1. Long-term deformations from left to right (a) autogenous shrinkage, drying shrinkage and (b) basic creep and drying creep specimens.

2.3.2. Compressive Tests

After the long-term tests, the cylinders were subjected to uniaxial compressive tests using an electromechanical machine with a capacity of 100 kN. A loading rate of 0.5 mm/min was considered. The displacement was measured in the same way as for creep tests by considering the two rings and 3 LVDT sensors as shown in Figure 1.

2.3.3. Acoustic Emission Monitoring

The compressive tests were monitored in parallel by means of AE technique. The AEWIN acquisition system with a data analysis and storage system was used. Eight R15a piezoelectric sensors were placed with a frequency range between 50 and 200 kHz and a resonance frequency of 150 kHz. Three sensors were put in the upper part and three others in the middle part (between the two rings) where each is 120° far from another as shown in Figure 2. The detected signals were amplified with a 40 dB differential amplifier. The detection threshold was set at 30 dB to avoid the effect of possible noise development.

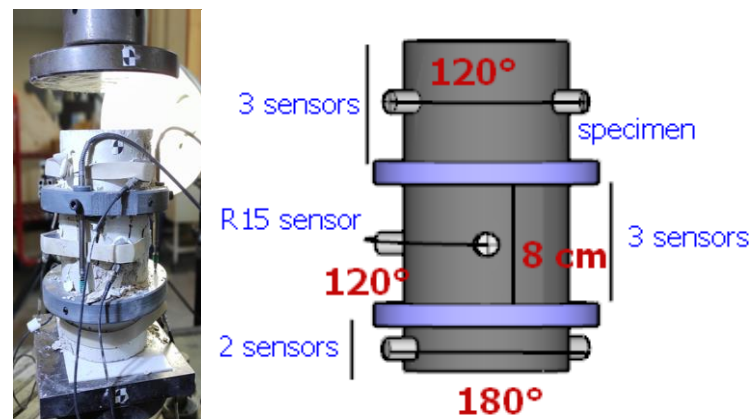


Figure 2. The compressive test setup and AE sensors' positions.

3. Results

The strain summation $\varepsilon_S(t)$ (Equation (4)) at time t of elastic strain $\varepsilon_{EL}(t)$, autogenous shrinkage $\varepsilon_{AS}(t)$, drying shrinkage $\varepsilon_{DS}(t)$ and basic creep strain $\varepsilon_{BC}(t)$, results generally in a total deformation, less than that obtained, at simultaneous drying, from a drying creep specimen $\varepsilon_{TD}(t)$ ($\varepsilon_{TD}(t)$ includes elastic strains $\varepsilon_{EL}(t)$ and total long-term deformations $\varepsilon_{TLTD}(t)$)

$$\varepsilon_S(t) = \varepsilon_{EL}(t) + \varepsilon_{AS}(t) + \varepsilon_{BC}(t) + \varepsilon_{DS}(t) \quad (4)$$

The difference between them represents the drying creep $\varepsilon_{DC}(t)$ (Equation (5)):

$$\varepsilon_{DC}(t) = \varepsilon_{TD}(t) - \varepsilon_S(t) \quad (5)$$

3.1. Long-Term Deformations

3.1.1. Shrinkage

Figure 3 shows the results of the mass loss, autogenous shrinkage and total shrinkage of NS and RS mixtures. Figure 3a presents the mass loss of both mixtures. The curves can be divided into three phases. A rapid mass loss is reported during the first days. Such a phase is controlled by the ambient conditions, and it continues as long as there is a supply of water from inside the specimen. Once the water migrating from the inside to the outside is not enough to meet that evaporative demand, the second phase starts and a lower rate of drying is observed in comparison to the first phase. The third phase is characterized by almost a constant low evaporation rate [32,33]. The mass loss values show a higher water migration rate for RS earth concrete mixtures. This may be related to its microstructure considering the additional porous network of RS and the water added for the pre-saturation.

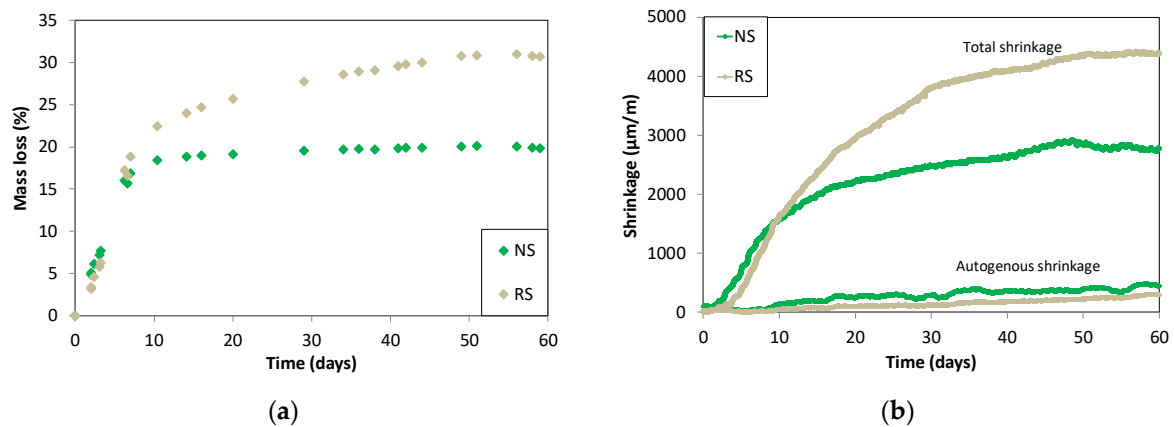


Figure 3. (a) The mass loss, (b) autogenous and total shrinkage of NS and RS earth concrete mixtures.

The autogenous shrinkage decreases when RS replaces NS. This tendency is similar to the trend reported for normal concrete [34,35]. This has been attributed to the internal curing effect of recycled aggregate. In fact, more water will flow out of the recycled concrete aggregate to compensate the water loss due to self-desiccation. Studies have found that a dry recycled concrete aggregate cannot effectively reduce the autogenous shrinkage [18]. The latter, even if additional water was added to the mixture, may be attributed to the absorption process that will take place by the recycled aggregate [36]. In the following study, the complete replacement of NS by RS following a pre-saturation of 80% reported a 54% decrease in the autogenous shrinkage of earth concrete. However, the drying shrinkage value of the RS mixture is higher, which may be attributed to the higher porosity of RS specimens in addition to the higher water absorption capacity [35,36].

Figure 4a shows the drying shrinkage (total shrinkage minus autogenous shrinkage) in parallel with the relative humidity and temperature. The temperature values did not show any great differences throughout the test, while the RH values did. As highlighted by arrows, a decrease in RH was accompanied by an increase in shrinkage rate.

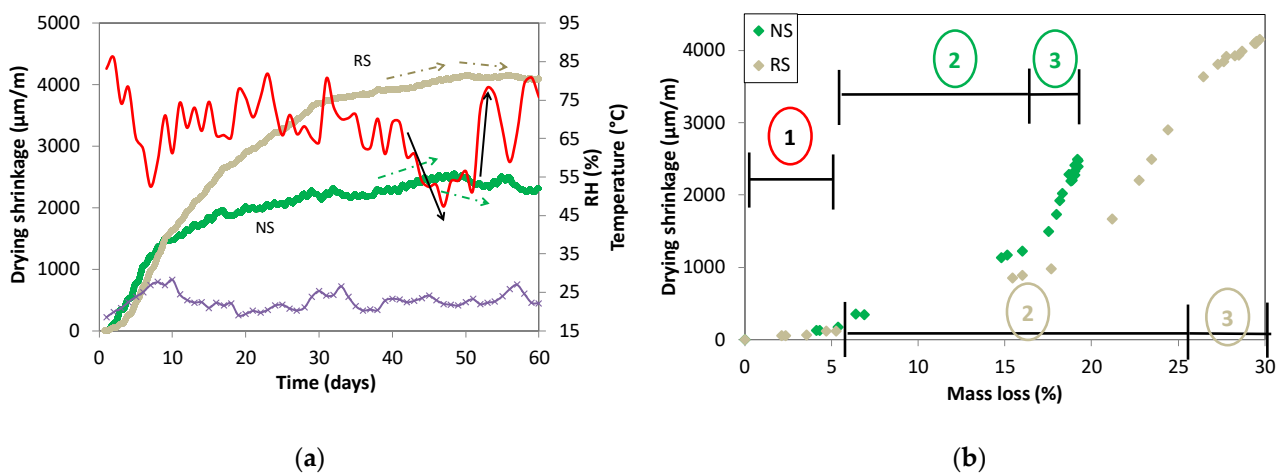


Figure 4. (a) The drying shrinkage in parallel with RH and temperature and (b) correlation between drying shrinkage and mass loss.

Figure 4b shows the drying shrinkage as function of mass loss. The complete replacement of NS by RS was reflected by an increase of drying shrinkage with a rate of 77% from 2313 µm/m to 4095 µm/m. The high mass loss values in the first phase were accompanied by low drying shrinkage rate as the migration of free water did not induce shrinkage [16,17]. The loss of water due to hydration may also contribute to this phenomenon [37], in addition to micro cracks [28]. In phases two and three, the mass loss was reflected by drying

shrinkage. It can be noticed that the rate of shrinkage in phase 2 is higher in the NS mixture, which may be due to different porosity network. Moreover, it has been observed that the three phases are longer in RS mixture, which may be attributed to the fact that the water migrated from RS specimen is not only the local water as for the NS specimen, but from the RS itself also due to pre-saturation [37].

3.1.2. Creep

Figure 5a shows the basic creep deformations $\varepsilon_{BC}(t)$ (after subtracting the elastic and autogenous shrinkage strains) and the total long-term deformations $\varepsilon_{TLTD}(t)$ (which are the deformations of drying creep specimen minus the elastic strains) of NS and RS mixtures. Figure 5b shows the specific basic creep, which is the basic creep deformation per unit stress. The results show that the basic creep increases with RS mixtures following the same tendency as that observed with ordinary concrete. It may be worthwhile to state that pre-saturation was carried out to RS in our study, while additional water was added rather than pre-saturation in other study [38], and both studies reported an increase of basic creep. Thus, this indicates that basic creep increases with recycled aggregate regardless of the way adopted for RS saturation.

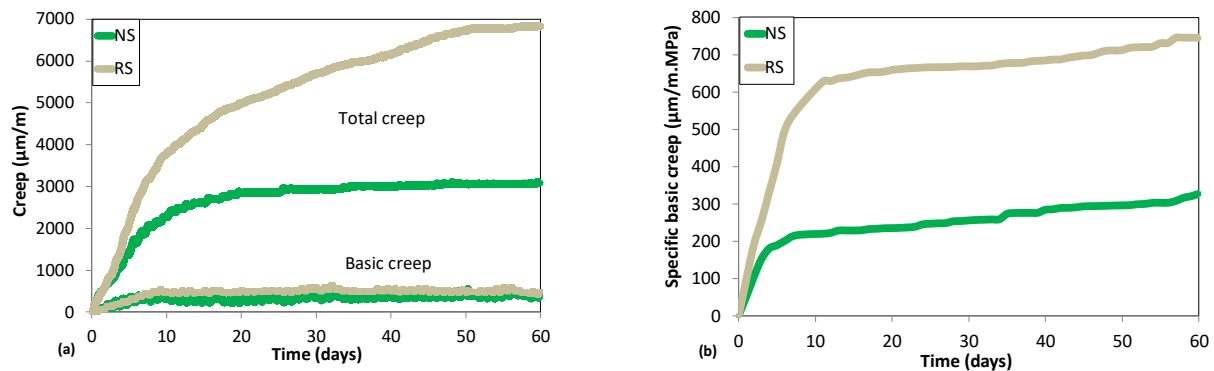


Figure 5. The basic creep and total long-term deformations (a) and specific basic creep (b) of NS and RS mixtures.

The hard grains hardly creep. Akono et al. [39], who declared higher basic creep tendencies in recycled aggregate concrete, verified that hard grains corresponded to almost 45% and 26% of the microstructure of natural aggregate concrete and recycled aggregate concrete, respectively. This validates the statement that the lower basic creep in NS earth concrete mixture may be attributed to a, probably, higher quantity of hard grains in its microstructure compared to RS mixture. Furthermore, creep can be caused by the transfer of water from micropores to macropores under a pressure [40]. Knowing that RS comprises of more water than NS and has different porosity distribution, more water may have been transferred to the larger pores due to the applied stress causing more of creep strain.

The total long-term deformation $\varepsilon_{TLTD}(t)$ also increases when RS replaces NS. While higher shrinkage in recycled aggregate mixtures is being attributed to porosity and water absorption [35], pore size distribution, lower elastic modulus [36], recycled aggregate source and particle size distribution [41], the total creep is being linked to those same factors [23]. For instance, Geng et al. [42] carried out a scanning electron microscope in order to show that recycled aggregate concrete is of higher porosity to justify its higher creep deformations.

In the following study, the replacement of NS by RS in earth concrete reported a 121% increase in $\varepsilon_{TLTD}(t)$ from 3085 to 6829 $\mu\text{m/m}$. Regarding basic creep, it increases by 12% from 445 to 500 $\mu\text{m/m}$ as RS replaces NS. On the other hand, knowing that RS specimen is of lower strength than NS specimen, it may be worthwhile to state that the basic creep per unit stress as shown in Figure 5b increases by 128% from 327 to 746 $\mu\text{m/m.MPa}$.

Figure 6 shows the strain summation $\epsilon_S(t)$ of the individual strains from one side (without elastic strain for a better verification of $\epsilon_{DC}(t)$) and $\epsilon_{TLTD}(t)$ related to DC specimen from other side. The difference between the two components represents $\epsilon_{DC}(t)$ or Picket’s effect. As already shown, $\epsilon_{BC}(t)$, $\epsilon_{DS}(t)$ and total $\epsilon_{TLTD}(t)$ increase while $\epsilon_{AS}(t)$ decreases when RS replaces NS. The replacement of NS by RS also increases the drying creep by 153% from 764 to 1935 $\mu\text{m}/\text{m}$. Regardless of the microstructural variations, it is important to highlight the microcracking effect. Due to drying, microcracks are formed on the surface of the specimen. Such cracks will not fully close and, thus, they are considered irreversible deformations. These deformations reduce the shrinkage of the specimen. RS drying specimens are more prone to develop drying cracks than NS, which is mainly due to the higher drying shrinkage [43]. The structural desiccation creep effect is linked to a reduction in microcracks generated by desiccation. Indeed, when a loaded drying specimen is assessed, the closure of cracks will take place on the planes normal to the direction of compression [13–15,22]. As more cracks would form on a non-loaded drying RS specimen, compressive loading will prevent the formation (or closing) of more cracks in RS than NS, and eventually lead to a higher additional drying creep strain in RS mixture.

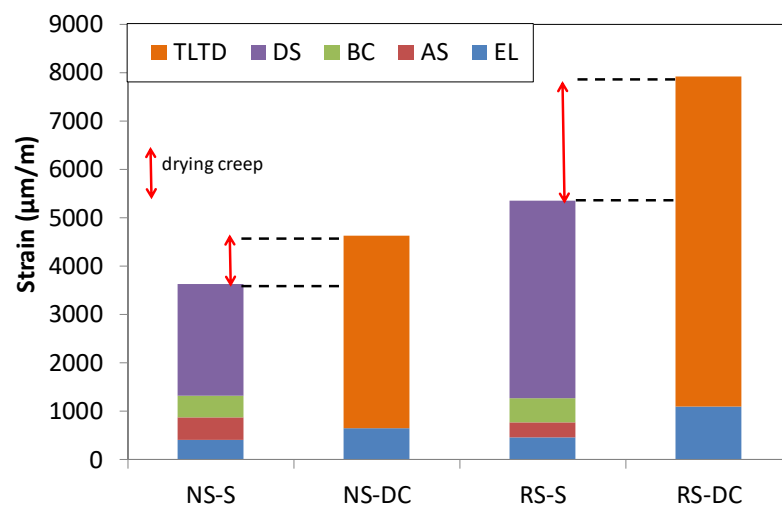


Figure 6. The evaluation of drying creep for NS and RS mixtures.

3.2. Strength Development Due to Long-Term Deformations

The specimens monitored under long term deformation were subjected to compressive tests after 60 days. The stress-strain curves are presented in Figure 7.

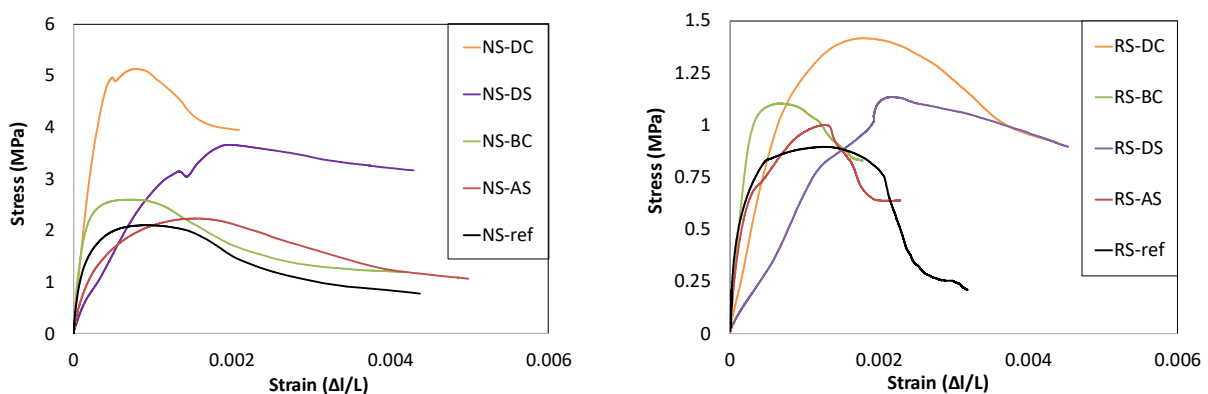


Figure 7. The stress-strain curves for NS and RS mixtures subjected to different loading and curing conditions.

Figure 8 shows the compressive strength and Young's modulus (or pre-peak slope) for NS and RS mixtures subjected to different loading and curing conditions, in addition to the compressive strength of the reference specimens (ref) measured at 28 days.

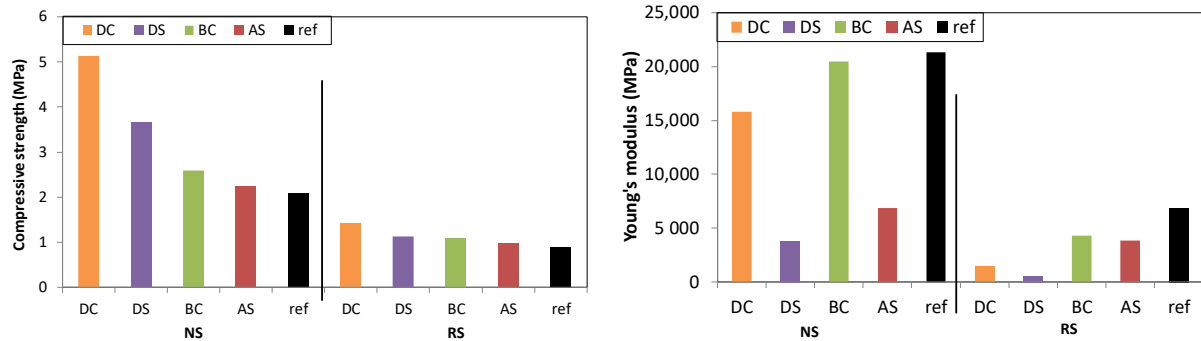


Figure 8. The compressive strength and Young's modulus for NS and RS mixtures subjected to different loading and curing conditions.

In both NS and RS mixtures, the compressive strength follows the same trend. From least to most, it is as follows: reference (ref) < autogenous shrinkage (AS) < basic creep (BC) < drying shrinkage (DS) < drying creep specimen (DC).

3.2.1. Reference Specimens

NS reported higher strength than RS. This is in agreement with the theoretical trend that declares degradation in the mechanical properties when RS replaces NS. The loss in strength in this study can be attributed to the higher porosity in addition to the increase in the initial water content represented by pre-saturation of RS.

3.2.2. Autogenous Shrinkage (AS) Specimens

Compared to the reference specimen, the AS specimens are of higher strength. While the reference tests were conducted at the age of 28 days, the compressive tests conducted on AS specimens were carried out at the age of 90 days. Therefore, the increase in strength can be attributed to the increase in the curing age period and thus better hydration. The strengths of NS and RS specimens increase by 11% and 6%, respectively.

3.2.3. Basic Creep (BC) Specimens

The BC specimens are of higher strength than AS specimens. The difference between these specimens is the external load and, thus, such an increase in strength can be attributed to consolidation and its consequences that involve water movement. Indeed, the applied load induces free water to flow and eventually rearrangement of soil particles takes place. This increases the solid-solid contacts at different positions and decreases the voids in the soil. This improvement in stiffening contributes to strength. The basic creep specimens reported 16% and 10% increases in strength in NS and RS compared to AS specimen, respectively. This may be attributed to the higher porosity of RS. As more voids and pores exist in the RS mixture, the resulted solid-solid contacts will be less important in RS mixture.

3.2.4. Drying Shrinkage (DS) Specimens

Due to the difference in relative humidity between the external and internal environments, the water migrates outside the specimen. The compressive strength may increase or decrease as a result of this water transfer. Based on the RH variations, and knowing that surface tension and interlayer water theories require RH less than 40% and 11%, respectively, the dominant mechanisms are, thus, the capillary and disjoining pressures; thus, soil gains strength by the combined actions of cohesion and friction [2]. The increase in these pressures, which are the sources of cohesion, leads to a stiffening effect. Such pressure increases link more of the gaps between the clay particles themselves, or the clays with

other grains' increasing frictions. On the other side, shrinkage may become restrained leading to the development of internal tensile stresses. If these stresses exceed the tensile strength of soil, microcracks are generated which may lead to strength loss. The increase in strength due to drying shows that the suction effect is the dominant phenomenon over the shrinkage induced cracking one. The increase in strength of the NS and RS drying shrinkage specimens reached 63% and 13%, respectively, compared to autogenous shrinkage specimens. This can indicate that more shrinkage induced cracking was formed in the RS mixture curbing the effect of suction. This, in addition, may support the hypothesis of microcracking effect regarding drying creep.

Compared to autogenous shrinkage specimens, the drying shrinkage ones revealed more increases in strength than the basic creep specimens. As the strength developments of both DS and BC specimens involve water movement, where the former is due to drying while the latter is due to external load, the higher increase of strength in DS specimen may be attributed to the more loss of water particles in the drying shrinkage specimen that led, eventually, to more solid-solid contacts and, thus, contributed more to strength.

3.2.5. Drying Creep (DC) Specimens

The strength in these specimens reported the highest value. With respect to AS specimens, the strengths of DC specimens increase by 129% and 42% for NS and RS specimens, respectively. Regardless of the intrinsic effect, the structural effect has to be highlighted as the rate of drying cracks and, more precisely, those who are on the planes normal to the compressive loading direction decreases [44].

As a compressive strength, the Young's modulus decreases with RS. However, the latter does not follow the same trend of the former. BC specimens reported the highest value. DC and BC specimens are of higher Young's modulus than DS and AS specimens, respectively. Thus, the loaded specimens are of higher Young's modulus than the unloaded specimens at the same curing condition. This basically intersects with the results of a previous study carried out on concrete beams [45]. The Young's modulus of DS for both specimens exhibited the lowest value, which may be due to shrinkage induced cracking. The lower modulus of elasticity of drying creep specimens compared to basic creep specimens confirms this deduction.

3.3. Acoustic Emission (AE) Analysis

Figure 9 shows the correlation between the stress and distribution of AE hits as functions of strain for NS and RS specimens subjected to different curing and loading conditions. The AE activity in RS specimens is lower than that of NS ones. This can be attributed to the lower strength of the former in addition to the porous state, possible defects and pre-saturation of RS that may have lowered its ITZ properties [2]. Note here that Saliba et al. [13–15] have showed a good correlation between creep displacement and the variation of the AE parameters with an important coupling between creep and damage during desiccation. In addition, the AE activity presented three regimes as that of the creep displacement, and three different mechanisms have been identified based on the quantitative analysis of the AE data [13–15]. Kouta et al. [17] showed that the AE technique can detect low energy processes during shrinkage of earth concrete as well as damage evolution. Different phases have been identified during drying indicating different mechanisms such as moisture/shrinkage gradients that develop at different depths in the specimens and by the presence of aggregates. The AE activity at the beginning of all mixtures can be attributed to the compaction taking place due to initial loadings. This phase demonstrates evidence for the closure of cracks and pores without the formation of new cracks. It can be seen that BC specimens exhibited lower AE activity in the pre-peak phase than the AS specimens. This can be attributed to several different aspects:

- The low Young's modulus in AS specimens will accommodate more stress buildup before cracking occurs [46]. This stress buildup will be accompanied by more AE signals.

- Fardoun et al. [2] monitored earth concrete specimens with AE under compressive tests at different curing ages and observed a reduction in AE activity with curing age and, thus with strength development. Therefore, the strength increase in the BC specimens will be reflected by lower pre-peak AE activity in addition to the Kaiser effect [13–15]
- The compaction phase exhibited lower AE in the specimen that was previously loaded during the durability tests (BC specimen); thus, such pre-loading acted as pre-compaction process [25].

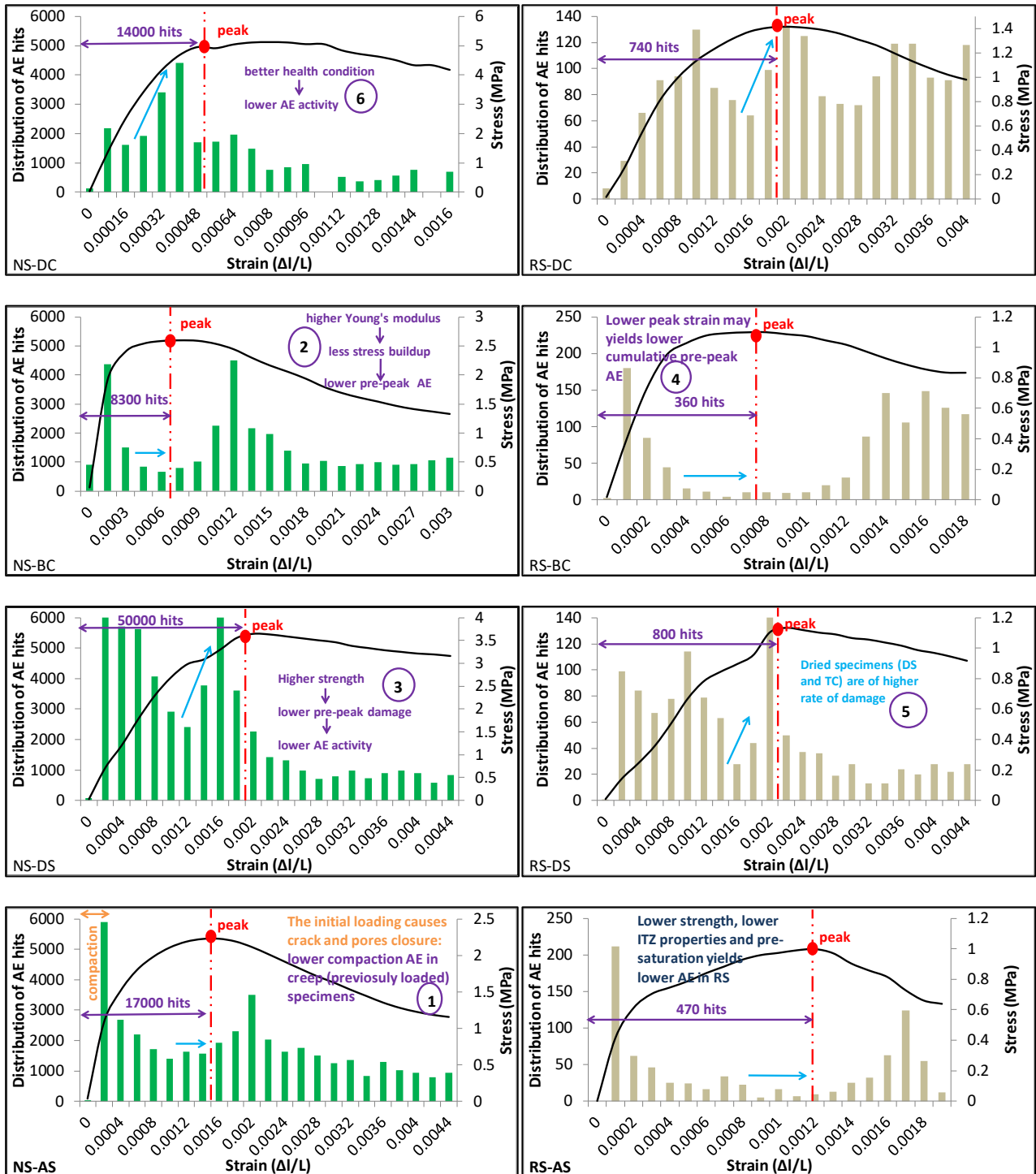


Figure 9. The correlation between the stress-strain curves and distribution of AE hits.

These four factors are valid between NS-DS and NS-DC from one side and between RS-DS and RS-DC specimens from the other side. Nevertheless, it was to a lower extent in RS specimens, which can be attributed to the less significant variations in strength and Young's modulus. DS and DC specimens reported the highest AE activity. This can indicate that AE reflected successfully:

- the suction effect where the particles got closer to each other, and thus higher friction takes place upon loading.
- the shrinkage induced cracking where friction along already existing drying cracks can take place upon loading.

This resulted friction based on the two processes will be accompanied by AE activity during the application of external stress. An increase in AE activity rate can be noticed for DS and DC specimens before the peak (as shown in sky blue arrows). This points out that these specimens exhibited a higher rate of damage directly before the peak than the sealed specimens (AS and BC). Thus, the dried specimens are more vulnerable to crack formation and propagation. It is worthwhile to state that DC specimens reported lower pre-peak AE activity than DS specimens due to the four aforementioned aspects (higher strength, higher Young's modulus, lower peak strain, and Kaiser effect).

Regarding the post peak phase, a more gradual increase of the AE activity can be noticed in the sealed specimens, in contrast with the ones that were subjected to drying and, thus, the former experienced less brittle behavior.

4. Conclusions and Perspectives

The long-term deformations of NS and RS earth concrete mixtures were evaluated. The residual properties of specimens subjected to different loading and curing conditions were also calculated and compressive tests were monitored in parallel with the AE technique. The followings can be stated:

- When RS completely replaces NS in earth concrete, the autogenous shrinkage decreases by 54% while the basic creep, drying shrinkage and drying creep increase by 12%, 77% and 153%, respectively.
- The compressive strength of the NS and RS specimens subjected to different loading and curing conditions increases as follows: reference < autogenous shrinkage < basic creep < drying shrinkage < drying creep specimen. In addition, NS mixtures reported higher strength development than RS ones except for autogenous shrinkage. The drying creep specimen reported 129% and 42% strength increase with respect to the autogenous shrinkage specimens in NS and RS, respectively.
- The loaded sealed and loaded drying specimens reported higher values of Young's modulus than the unloaded sealed and unloaded drying specimens, respectively. The basic creep specimens exhibited the highest value of Young's modulus while the drying shrinkage specimens reported the lowest value, which may be attributed to shrinkage induced cracking.
- The generation of AE activity in the pre-peak phase is influenced by compressive strength, Young's modulus, drying process, peak strain and loading. Furthermore, it can be stated that the monitoring of AE activity during the compressive tests reflected the vulnerability of specimens subjected to drying due to shrinkage induced cracking. Moreover, the sealed specimens evidenced less brittle behavior than the dry ones according to AE.

Additional studies will be realized in the future in order to study the effect of different loading levels on creep behavior and take into account the variability of the soil. Additional tests will be also realized at the microscopic level, in addition to the classification of AE signals in order to better understand the different mechanisms and evaluate, for example, the vulnerability to drying and ITZ properties. Finally, the effect of recycled aggregates surface treatments on their compatibility and functionality in the earth concrete mix will be studied, in addition to the investigation of their thermal insulation properties.

Author Contributions: Conceptualization, J.S.; data curation, H.F.; formal analysis, H.F. and J.S.; funding acquisition, N.S.; investigation, H.F. and J.S.; methodology, J.S., J.-L.C. and N.S.; project administration, N.S.; resources, J.S., J.-L.C., A.C. and N.S.; supervision, J.S. and N.S.; validation, J.S.; writing—original draft, H.F.; writing—review and editing, J.S. All authors have read and agreed to the published version of the manuscript.

Funding: This research received no external funding.

Institutional Review Board Statement: The study did not require ethical approval.

Informed Consent Statement: Not applicable.

Data Availability Statement: Not applicable.

Acknowledgments: Not applicable.

Conflicts of Interest: The authors declare no conflict of interest.

References

1. van Damme, H.; Houben, H. Earth concrete. Stabilization revisited. *Cem. Concr. Res.* **2018**, *114*, 90–102. [CrossRef]
2. Fardoun, H.; Saliba, J.; Saiyouri, N. Evolution of acoustic emission activity throughout fine recycled aggregate earth concrete under compressive tests. *Theor. Appl. Fract. Mech.* **2022**, *119*, 103365. [CrossRef]
3. Kouta, N.; Saliba, J.; Saiyouri, N. Effect of flax fibers on early age shrinkage and cracking of earth concrete. *Constr. Build. Mater.* **2020**, *254*, 119315. [CrossRef]
4. Ngo, D.C.; Saliba, J.; Saiyouri, N.; Sbartai, Z.M. Design of a soil concrete as a new building material—Effect of clay and hemp proportions. *J. Build. Eng.* **2020**, *32*, 101553. [CrossRef]
5. Kouta, N.; Saliba, J.; Saiyouri, N. Fracture behavior of flax fibers reinforced earth concrete. *Eng. Fract. Mech.* **2020**, 107378. [CrossRef]
6. Kabirifar, K.; Mojtahedi, M.; Wang, C.C.; Tam, V.W.Y. Effective construction and demolition waste management assessment through waste management hierarchy; a case of Australian large construction companies. *J. Clean. Prod.* **2021**, *312*, 127790. [CrossRef]
7. Vegas, I.; Broos, K.; Nielsen, P.; Lambertz, O.; Lisbona, A. Upgrading the quality of mixed recycled aggregates from construction and demolition waste by using near-infrared sorting technology. *Constr. Build. Mater.* **2015**, *75*, 121–128. [CrossRef]
8. Ni, S.; Liu, H.; Li, Q.; Quan, H.; Gheibi, M.; Fathollahi-Fard, A.M.; Tian, G. Assessment of the engineering properties. carbon dioxide emission and economic of biomass recycled aggregate concrete: A novel approach for building green concretes. *J. Clean. Prod.* **2022**, *365*, 132780. [CrossRef]
9. Zhang, C.; Hu, M.; Dong, L.; Gebremariam, A.; Miranda-Xicotencatl, B.; di Maio, F.; Tukker, A. Eco-efficiency assessment of technological innovations in high-grade concrete recycling. *Resour. Conserv. Recycl.* **2019**, *149*, 649–663. [CrossRef]
10. Nedeljković, M.; Visser, J.; Šavija, B.; Valcke, S.; Schlangen, E. Use of fine recycled concrete aggregates in concrete: A critical review. *J. Build. Eng.* **2021**, *38*, 102196. [CrossRef]
11. Arrigoni, A.; Beckett, C.T.S.; Ciancio, D.; Pelosato, R.; Dotelli, G.; Grillet, A.C. Rammed Earth incorporating Recycled Concrete Aggregate: A sustainable, resistant and breathable construction solution. *Resources Conserv. Recycl.* **2018**, *137*, 11–20. [CrossRef]
12. Kanema, J.M.; Eid, J.; Taibi, S. Shrinkage of earth concrete amended with recycled aggregates and superplasticizer: Impact on mechanical properties and cracks. *Mater. Des.* **2016**, *109*, 378–389. [CrossRef]
13. Saliba, J.; Loukili, A.; Grondin, F.; Regoin, J.P. Identification of damage mechanisms in concrete under high level creep by the acoustic emission technique. *Mater. Struct.* **2014**, *47*, 1041–1053. [CrossRef]
14. Saliba, J.; Grondin, F.; Loukili, A. Coupling creep and damage in concrete under high sustained loading. In Proceedings of the International Conference on Fracture Mechanics of Concrete and Concrete Structures, Framcos-7, Jeju, Korea, 23–28 May 2010.
15. Saliba, J.; Loukili, A.; Grondin, F. 6—Acoustic emission monitoring and quantitative evaluation of damage in concrete beams under creep. In *Acoustic Emission and Related Non-Destructive Evaluation Techniques in the Fracture Mechanics of Concrete*, 2nd ed.; Woodhead Publishing: Sawston, UK, 2015; pp. 115–137. [CrossRef]
16. Saliba, J.; Rozière, E.; Grondin, F.; Loukili, A. Influence of shrinkage-reducing admixtures on plastic and long-term shrinkage. *Cem. Concr. Comps.* **2011**, *33*, 209–217. [CrossRef]
17. Kouta, N.; Saliba, J.; Saiyouri, N. Monitoring of earth concrete damage evolution during drying. *Constr. Build. Mater.* **2021**, *313*, 125340. [CrossRef]
18. Eurostat, Recovery Rate of Construction and Demolition Waste. 2022. Available online: https://ec.europa.eu/eurostat/databrowser/view/cei_wm040/default/table (accessed on 27 October 2021).
19. Mao, Y.; Liu, J.; Shi, C. Autogenous shrinkage and drying shrinkage of recycled aggregate concrete: A review. *J. Clean. Prod.* **2021**, *295*, 126435. [CrossRef]
20. Kanema, J.M. The influence of soil content on the mechanical properties, drying shrinkage and autogenous shrinkage of earth concrete. *J. Build. Eng.* **2017**, *13*, 68–76. [CrossRef]

21. Chen, Z.-J.; Feng, W.-Q.; Yin, J.-H. A new simplified method for calculating short-term and long-term consolidation settlements of multi-layered soils considering creep limit. *Comput. Geotech.* **2021**, *138*, 104324. [[CrossRef](#)]
22. Le, T.M.; Fatahi, B.; Khabbaz, H. Viscous Behaviour of Soft Clay and Inducing Factors. *Geotech. Geol. Eng.* **2012**, *30*, 1069–1083. [[CrossRef](#)]
23. Rahimi-Aghdam, S.; Bazant, Z.P.; Cusatis, G. Extended Microprestress-Solidification Theory (XMPS) for Long-Term Creep and Diffusion Size Effect in Concrete at Variable Environment (No. 18-04/33788r). *J. Eng. Mech.* **2018**, *145*. [[CrossRef](#)]
24. Sinko, R.; Bažant, Z.P.; Keten, S. A nanoscale perspective on the effects of transverse microprestress on drying creep of nanoporous solids. *Proc. R. Soc. A* **2018**, *474*, 20170570. [[CrossRef](#)]
25. Bazant, Z.P.; Chern, J.C. Concrete creep at variable humidity: Constitutive law and mechanism. *Mater. Struct.* **1985**, *18*, 1–20. [[CrossRef](#)]
26. Lye, C.-Q.; Dhir, R.K.; Ghataora, G.S.; Li, H. Creep strain of recycled aggregate concrete. *Constr. Build. Mater.* **2016**, *102*, 244–259. [[CrossRef](#)]
27. Bui, Q.-B.; Morel, J.C. The creep of Rammed Earth material. In *Rammed Earth Construction and Structures*; Taylor & Francis: Abingdon, UK, 2015.
28. Boniface, A.; Saliba, J.; Sbartai, Z.M.; Ranaivomanana, N.; Balaýssac, J.P. Evaluation of the acoustic emission 3D localisation accuracy for the mechanical damage monitoring in concrete. *Eng. Fract. Mech.* **2020**, *223*, 106742. [[CrossRef](#)]
29. *XP P94-041*; Reconnaissance and Testing—Size Identification—Wet Sieving Method. Association Francaise de Normalisation AFNOR Standard: Saint-Denis, France, 1995.
30. *NF P94-057*; Reconnaissance and Testing—Particle Size Analysis—Sedimentation Method. Association Francaise de Normalisation AFNOR Standard: Saint-Denis, France, 1992.
31. *NF EN197-1*; Composition, Specifications and Conformity Criteria of Common Cements. Association Francaise de Normalisation AFNOR Standard: Saint-Denis, France, 2012.
32. Quattrone, M.; Cazacliu, B.; Angulo, S.C.; Hamard, E.; Cothenet, A. Measuring the water absorption of recycled aggregates, what is the best practice for concrete production? *Constr. Build. Mater.* **2016**, *123*, 690–703. [[CrossRef](#)]
33. An, N.; Hemmati, S.; Cui, Y.; Tang, C. Numerical investigation of water evaporation from Fontainebleau sand in an environmental chamber. *Eng. Geol.* **2018**, *234*, 55–64. [[CrossRef](#)]
34. Tran, D.K.; Ralaizafisoarivony, N.; Charlier, R.; Mercatoris, B.; Léonard, A.; Toye, D.; Degré, A. Studying the effect of desiccation cracking on the evaporation process of a Luvisol—From a small-scale experimental and numerical approach. *Soil Tillage Res.* **2019**, *193*, 142–152. [[CrossRef](#)]
35. Bravo, M.; de Brito, J.; Evangelista, L.; Pacheco, J. Durability and shrinkage of concrete with CDW as recycled aggregates: Benefits from superplasticizer’s incorporation and influence of CDW composition. *Constr. Build. Mater.* **2018**, *168*, 818–830. [[CrossRef](#)]
36. Silva, R.V.; de Brito, J.; Dhir, R.K. Prediction of the shrinkage behavior of recycled aggregate concrete: A review. *Constr. Build. Mater.* **2015**, *77*, 327–339. [[CrossRef](#)]
37. Samouh, H.; Rozière, E.; Loukili, A. The differential drying shrinkage effect on the concrete surface damage: Experimental and numerical study. *Cem. Concr. Res.* **2017**, *102*, 212–224. [[CrossRef](#)]
38. Fan, Y.; Niu, H.; Zhang, X. Impact of the properties of old mortar on creep prediction model of recycled aggregate concrete. *Constr. Build. Mater.* **2020**, *239*, 117772. [[CrossRef](#)]
39. Akono, A.-T.; Chen, J.; Zhan, M.; Shah, S.P. Basic creep and fracture response of fine recycled aggregate concrete. *Constr. Build. Mater.* **2021**, *26*, 121107. [[CrossRef](#)]
40. Mitchell, J.K.; Soga, K. *Fundamentals of Soil Behaviour*, 3rd ed.; Wiley: New York, NY, USA, 2005.
41. Li, Z.; Liu, J.; Xiao, J.; Zhong, P. Internal curing effect of saturated recycled fine aggregates in early-age mortar. *Cem. Concr. Compos.* **2020**, *108*, 103444. [[CrossRef](#)]
42. Geng, Y.; Zhao, M.; Yang, H.; Wang, Y. Creep model of concrete with recycled coarse and fine aggregates that accounts for creep development trend difference between recycled and natural aggregate concrete. *Cem. Concr. Compos.* **2019**, *103*, 303–317. [[CrossRef](#)]
43. Ideker, J.H.; Tanner, J.E.; Adams, M.P.; Jones, A. *Durability Assessment of Recycled Concrete Aggregates for use in New Concrete: Phase II Report*; Oregon Transportation and Education Consortium: Portland, OR, USA, 2014; p. 98.
44. Yurtdas, I.; Burlion, N.; Skoczylas, F. Experimental characterisation of the drying effect on uniaxial mechanical behaviour of mortar. *Mater. Struct.* **2004**, *37*, 170–176. [[CrossRef](#)]
45. Asamoto, S.; Kato, K.; Maki, T. Effect of creep induction at an early age on subsequent prestress loss and structural response of prestressed concrete beam. *Constr. Build. Mater.* **2014**, *70*, 158–164. [[CrossRef](#)]
46. Adams, M.P.; Fu, T.; Cabrera, A.G.; Morales, M.; Ideker, J.H.; Isgor, O.B. Cracking susceptibility of concrete made with coarse recycled concrete aggregates. *Constr. Build. Mater.* **2016**, *102*, 802–810. [[CrossRef](#)]